JOURNAL OF GEOPHYSICAL RESEARCH, VOL. 105, NO. A1, PAGES 61–78, JANUARY 1, 2000

# Characteristics of energetic (≳30 keV/nucleon) ions observed by the Wind/STEP instrument upstream of the Earth's bow shock

M. I. Desai, G. M. Mason,[1] and J. R. Dwyer
Department of Physics, University of Maryland, College Park

J. E. Mazur
Aerospace Corporation, Los Angeles, California

T. T. von Rosenvinge and R. P. Lepping
NASA Goddard Space Flight Center, Greenbelt, Maryland

**Abstract.** We investigate here the characteristics of energetic ions (0.03–2.0 MeV/nucleon) during 1225 upstream events observed by the Energetic Particles: Anisotropy, Composition, and Transport/Suprathermal Energetic Particle (EPACT/STEP) instrument on board the Wind spacecraft from 1994 day 325 to 1999 day 92. We find that (1) the event occurrence rate showed significant variations with changes in the solar cycle, (2) the occurrence rate increased when both the solar wind speed and the geomagnetic activity index were enhanced, (3) most events were observed within $\pm 80\ R_E$ in $Y_{GSE}$ and inside $\sim 100\ R_E$ in $X_{GSE}$, although the events occurred at all locations of the Wind orbit, (4) ~73% of the events were observed when the interplanetary magnetic field was radial and in the ecliptic plane, and when the spacecraft was most likely magnetically connected to the bow shock, (5) the events lasted typically between 10 min to 3 hours and exhibited strong sunward field-aligned flow, (6) ~25% of the ion events were accompanied by 20–48 keV electrons as measured by the Wind/3DP instrument, (7) the energy spectra 100–300 keV protons and 30–300 keV/nucleon He-Fe during ~70% of the events obeyed power laws with $\gamma$ between 3 and 5, while the energy spectra of He and CNO for ~30% of the events softened above ~80 keV/nucleon obeyed power laws with $\gamma$ ~3–5, (8) the total energy ion spectrum above ~0.5 MeV energy was dominated by heavier ions during the events, (9) a substantial fraction (≳40%) of the spectra for all species extended above ~150 keV/*e*, and (10) the heavy ion composition of the events was similar to typical solar wind values. We compare the above findings with the main predictions of the magnetospheric leakage and the Fermi acceleration models and find that neither model can satisfactorily account for our results. We highlight the new challenges and requirements for both models.

## 1. Introduction

Energetic ions with energies ranging from a few keV up to 1–2 MeV have been routinely observed upstream of the Earth's bow shock since the 1960s [e.g., *Asbridge et al*., 1968; *Lin et al*., 1974; *Sarris et al*., 1976; *Scholer et al*., 1979]. Most of the measurements obtained within ~25 $R_E$ of the bow shock were explained in terms of either (1) the leakage of magnetospheric particles accelerated within the Earth's plasma sheet during substorms into the upstream region [e.g., *Sarris et al*., 1976; *Krimigis et al*., 1978] or (2) the acceleration of solar wind ions either via reflection at the quasi-perpendicular portions of the bow shock [*Sonnerup*, 1969; *Gosling et al*., 1978] or via scattering by the waves (i.e., the first-order Fermi process) prevalent near the quasi-parallel portion of the shock [e.g., *Scholer et al*., 1981a; *Lee*, 1982]. The ions near the quasi-parallel bow shock are commonly known as diffuse ions [*Gosling et al*., 1978].

The main characteristics of ion events originating from inside the magnetosphere as outlined by *Sarris et al*. [1976] and *Anagnostopoulos et al*. [1986] are (1) the total energy ion spectrum (presumed to be dominated by protons) typically extends above ~300 keV up to ~1–2 MeV in energy, (2) the energy spectrum either obeys a power law at all energies or has a characteristic hump between 100 and 300 keV, (3) all types of velocity dispersion are observed during the onsets of the events, (4) the ion angular distributions exhibit large anisotropies due to either field-aligned flows or spatial density gradients, (5) the ions are often accompanied by energetic (≳30 keV) electrons, and (6) the events usually occur in conjunction with intense geomagnetic activity.

In contrast, the main characteristics of diffuse ions measured within ~10 $R_E$ of the bow shock as outlined by *Gosling et al*. [1978], *Ipavich et al*. [1981a, b], and *Scholer et al*. [1981a] are (1) the ion energy spectrum rarely extends above ~150 keV/*e*, (2) the energy spectrum behaves as an exponential in energy/charge, (3) the intensity of ~30 keV protons decreases with increasing distance from the bow shock, (4) the ions are never

[1]Also at Institute for Physical Science and Technology, University of Maryland, College Park.



Paper number 1999JA900406.
0148-0227/00/1999JA900406$09.00

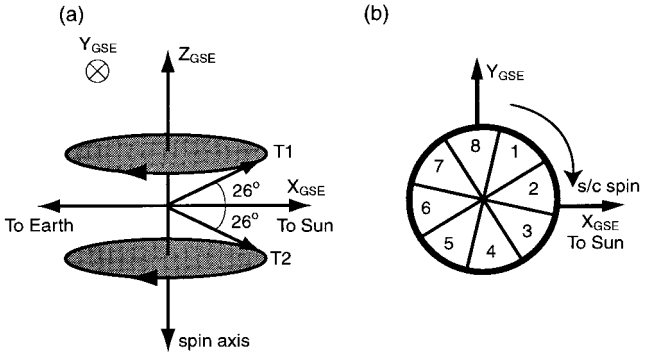


**Figure 1.** (a) Look directions of the two telescopes (T1 and T2) of the Suprathermal Energetic Particle (STEP) instrument of the Energetic Particles: Anisotropy, Composition, and Transport (EPACT) investigation [*von Rosenvinge et al*., 1995] on board the Wind spacecraft in the $XZ$ plane in the Geocentric Solar Ecliptic (GSE) coordinate system. (b) Orientation of all the sectors (labeled 1–8) of T1 and T2, as viewed from above the $XY$ or the ecliptic plane.

accompanied by energetic electrons, (5) the ion angular distributions are nearly isotropic, (6) the onset phases of the events exhibit inverse velocity dispersion, and (7) the ions are typically accompanied by large amplitude low-frequency waves.

However, despite the apparent distinction between the two types of events, the origin of upstream ions near Earth has remained controversial because first, it is not known how the energy spectra of the magnetospheric ions behave in the 50–200 keV energy range, i.e., the energy regime where the two types of events overlap. Second, the lower-energy magnetospheric ions could get scattered by the upstream waves and acquire nearly isotropic distributions which renders them virtually indistinguishable from the diffuse ion population. Indeed, ions such as $O^+$, which originate from the Earth's ionosphere (solar wind oxygen ions typically have higher charge states), have occasionally been observed during diffuse ion events [*Möbius et al*., 1986].

Thus, on the one hand, *Scholer et al*. [1981a, 1990] have championed the existence of two distinct origins for the $\lesssim$200 keV energy ions in upstream events, namely, those of magnetospheric origin and those accelerated at the bow shock. While, on the other hand, using simultaneous multispacecraft measurements obtained inside the Earth's magnetotail, magnetosheath, and upstream of the bow shock, *Sarris et al*. [1978], *Krimigis et al*. [1978], and *Anagnostopoulos et al*. [1986] have claimed that the majority of the energetic ($\gtrsim$50 keV) ions, whether they show characteristics similar to diffuse ions or not, are of magnetospheric origin, and that Fermi acceleration at the bow shock plays an insignificant role in their production. Thus the disagreements regarding the origin of upstream ions have been focused primarily on the relative contributions of magnetospheric and bow shock accelerated ions to the particle populations.

The situation further upstream ($\gtrsim 30\ R_E$) of the bow shock is even more complex because most of the events exhibit (1) large (100:1) field-aligned anisotropies, implying scatter-free transport, and (2) little or no velocity dispersion during their onset or decay phases, indicating the convection of spatial structures populated with the upstream particles over the spacecraft [*Sanderson et al*., 1981; *Scholer et al*., 1981b]. These measurements alone conveyed little information regarding the origin of the upstream ions because low-energy particles were generally found to propagate essentially scatter-free once they were outside the ion foreshock region where pitch angle scattering by the upstream waves is more conducive [e.g., *Mitchell et al*., 1983].

The key measurement that has not been available until the launch of high-sensitivity mass spectrometers on board the Wind spacecraft in November 1994 is the energetic ($\gtrsim$75 keV/nucleon) heavy ion composition of upstream events. The elemental abundances should provide new insights into the dilemma of the origin of these particles, since the ion composition of the two potential sources of the parent populations, i.e., the Earth's magnetosphere and the solar wind, are considerably different. An early analysis [*Mason et al*., 1996] showed that the ion composition of some upstream events observed at Wind was similar to that measured in corotating interaction regions (CIRs) that were formed when high-speed ($\sim$600–750 km $s^{-1}$) solar wind streams interacted with slower ($\sim$300–450 km $s^{-1}$) solar wind streams. A study by *Dwyer et al*. [1997] showed that the ion composition, specifically the enhancement of $^3$He, during some of the events was similar to that measured during a solar energetic particle (SEP) event that had occurred a few hours earlier. These results were interpreted as evidence for further acceleration of an energetic seed population (provided by CIRs or SEPs) at the bow shock, although strictly speaking they could not rule out acceleration of these seed populations in the magnetosphere with subsequent leakage into the upstream medium.

In this paper we present a detailed statistical analysis of the durations, the energetic electron association, and the angular distributions, the energy spectra and the elemental abundances of energetic ($\gtrsim$30 keV/nucleon) heavy ions during 1225 upstream events observed at Wind from 1994 day 325 to 1999 day 92. Our survey also includes an analysis of the temporal and spatial occurrence rates of the events, and the magnetospheric and interplanetary (i.e., the magnetic field orientation and the solar wind speed) conditions during the events. We compare our findings with the main predictions of the magnetospheric leakage and the Fermi acceleration models and highlight the new challenges posed by our results for both models.

## 2. Instrumentation

We use energetic ($\gtrsim$30 keV/nucleon) ion data from the Suprathermal Energetic Particle (STEP) instrument of the Energetic Particles: Anisotropy, Composition, and Transport (EPACT) investigation [*von Rosenvinge et al*., 1995] on board the Wind spacecraft. The STEP instrument uses time-of-flight and residual energy measurements to identify elements over the range He-Fe in the 0.03–2 MeV/nucleon energy range in two identical telescopes (named T1 and T2), each with a geometrical factor of 0.4 $cm^2$ sr and a rectangular field of view with an angular acceptance of 44° in azimuth and 17° in polar angle. The instrument also identifies 0.1–2.5 MeV protons. Thus, in terms of the heavy ion energy spectra and the elemental abundances, STEP has provided us with important new information regarding the upstream events.

Figure 1a shows that T1 and T2 are oriented at 64° and 116°, respectively to the spacecraft spin axis, which points along the $-Z$ axis in the Geocentric Solar Ecliptic (GSE) coordinate system. In this system, the $+X$ axis points from the Earth toward the Sun, the $+Z$ axis points along the normal to the ecliptic plane, and the $+Y$ axis, which lies in the ecliptic plane,

completes a right-handed set. During each spacecraft spin the two telescopes sweep out sections of interplanetary space just above and below the $XY$ or the ecliptic plane. The scan planes of both telescopes are divided into eight azimuthal sectors of 45° each. Figure 1b shows the layout of the eight sectors of T1 (and T2) as viewed from above the ecliptic plane. Although the orientation of a particular sector relative to the $+X$ and $+Y$ axes depends on the location of the spacecraft in the $XY$ plane at that time, in general, sectors 5–8 of both T1 and T2 measure particles arriving from the Earth, while sectors 1–4 detect particles flowing away from the Sun.

To aid our analysis, we have also used data from the Solar Wind Plasma Experiment (SWE) [*Ogilvie et al*., 1995], the Magnetic Field Investigation (MFI) [*Lepping et al*., 1995], and energetic (20–48 keV) electron data from the three-dimensional plasma (3DP) instrument [*Lin et al*., 1995] on board the Wind spacecraft. In addition, we obtained the geomagnetic activity index, $K_P$, from www.ngdc.noaa.gov:80/stp/geomag/.

## 3. Event Selection Criteria

We have used the 96-s spin-averaged 40–80 keV/nucleon C + N + O intensity (hereinafter referred to as the 60 keV/nucleon CNO intensity) measured by STEP to identify 1225 upstream events from 1994 day 325 to 1999 day 92. As an example of the data, Plate 1 shows the 60 keV/nucleon CNO intensity from 1995 day 32 to day 37. All events were selected on the basis of the following: (1) abrupt (of the order of a few minutes) increases in the CNO intensity above 5 particles $(\text{cm}^2\ \text{s sr MeV/nucleon})^{-1}$; this threshold is denoted by the dashed horizontal line in Plate 1, (2) the event duration time should be greater than 3 min, (3) two or more intensity enhancements within 30 min were considered as the same event, (4) the mean CNO intensity measured in sectors 5–8 in the solar wind frame should be higher than that measured in sectors 1–4 for both telescopes, and (5) the event should have occurred at a radial distance $R > 20\ R_E$ from the Earth. We remark that although all the selected events were accompanied by appreciable enhancements in the 100–160 keV proton intensity, all the proton enhancements were not necessarily accompanied by enhancements in the CNO intensity above the required minimum threshold. However, in using proton enhancements to select upstream events, the total number of events increases by only ~10%, and that even these additional events were in fact accompanied by substantial increases in the heavier ion intensities. An example of such an event occurred at ~0730 UT on day 32 and is marked A in Plate 1.

During the 5-day period shown in Plate 1, we found that 12 events (numbered 1–12 and identified by the shaded vertical bands) satisfied the above five criteria. Note that although event 10 consists of more than two enhancements, criterion 3 has ensured that they were considered as a single event. Furthermore, since criterion 2 excludes events which lasted <3 min (e.g., the enhancement marked B at ~2230 UT on day 32), our analysis is actually based on a lower limit for the number of events. Nonetheless, both these criteria are quite appropriate because, in general, longer averaging periods are needed to obtain sufficient counting statistics to compute the energy spectra and the relative abundances of the heavier ions. We remark that the intensity enhancement marked C at ~1250 UT on day 35 was not included here because the mean intensity measured in sectors 1–4 in both telescopes during the event was higher than that measured in sectors 5–8. Upstream events with substantial fluxes from the sunward direction have also been observed by the Ultra-Low-Energy Isotope Spectrometer (ULEIS) [*Mason et al*., 1998a], on board the Advanced Composition Explorer (ACE, launched in August 1997), and are discussed by *Dwyer et al*. [1999].

## 4. Characteristics of a Typical Upstream Event

### 4.1. Time-Intensity Profiles

Plate 2 shows 96-s spin-averaged intensities of 100–450 keV protons, 30–160 keV/nucleon He, 30–160 keV/nucleon CNO, 20–80 keV/nucleon NeS, and 20–80 keV/nucleon Fe measured by STEP from 0800 to 1200 UT on day 34, 1995. This 4-hour interval includes event 8 shown in Plate 1. Only those channels which detected an appreciable intensity enhancement during the event are shown. During this event the higher-energy channels for all species showed no intensity increases above the preevent background. On this day, Wind was ~200 $R_E$ upstream of the Earth.

From Plate 2 we note that (1) the H, He, and CNO intensities increase and decrease abruptly and nearly simultaneously at all energies, indicating the lack of velocity dispersion (i.e., time delays ≳2 min) during the onset and decay phases, and (2) the H, He, CNO, and NeS intensities at all energies remain relatively steady for almost 20 min starting from ≈0930 UT, while the Fe intensities at both energies appear to peak at ≈0945 UT. We remark that while there are marked differences in the time-intensity profiles from event to event, event 8 does provide an excellent example of a typical upstream event from the perspective of the measurements of STEP.

### 4.2. Pitch Angle Distributions

Figure 2 shows the pitch angle distributions of 120–160 keV protons, and 40–80 keV/nucleon He ions measured in the solar wind frame in (left) T1 and (right) T2 during event 8. The intensities are obtained by performing a Compton-Getting transformation [*Ipavich*, 1974] on the measured intensities using the solar wind plasma data and the sector orientation shown in Figure 1. The pitch angles in the solar wind frame are derived similarly from the look directions of the sectors with respect to the orientation of the magnetic field. Since the magnetic field components remained relatively steady throughout event 8, we carried out the above calculations for each 10-min interval from 0920 to 1030 UT, and then averaged the data over the 70-min interval. The intensity measured in each sector is normalized to the maximum intensity during the interval and plotted versus the corresponding pitch angle.

Figure 2 shows that both protons and He ions exhibit strong (≳100:1) anisotropies with intensity maxima at pitch angles ≲45° in sector 7 of both telescopes, indicating a dominant field-aligned flow away from the Earth. Note that these values are not exactly 0° because we have assumed that the look direction of the sectors are along their respective centerlines. We also note from Figure 2 that the angular distribution of ~160 keV protons is relatively broader than that of the ~60 keV/nucleon He ions, i.e., a substantial fraction of the protons have pitch angles between 60° and 120°. We remark that the angular distributions of CNO and Fe (not shown) also exhibit strong field-aligned flow away from the Earth during this event.

### 4.3. Energy Spectra

In analyzing some of the upstream events observed by STEP during 1994 and 1995 (i.e., a small subset of the events ana-

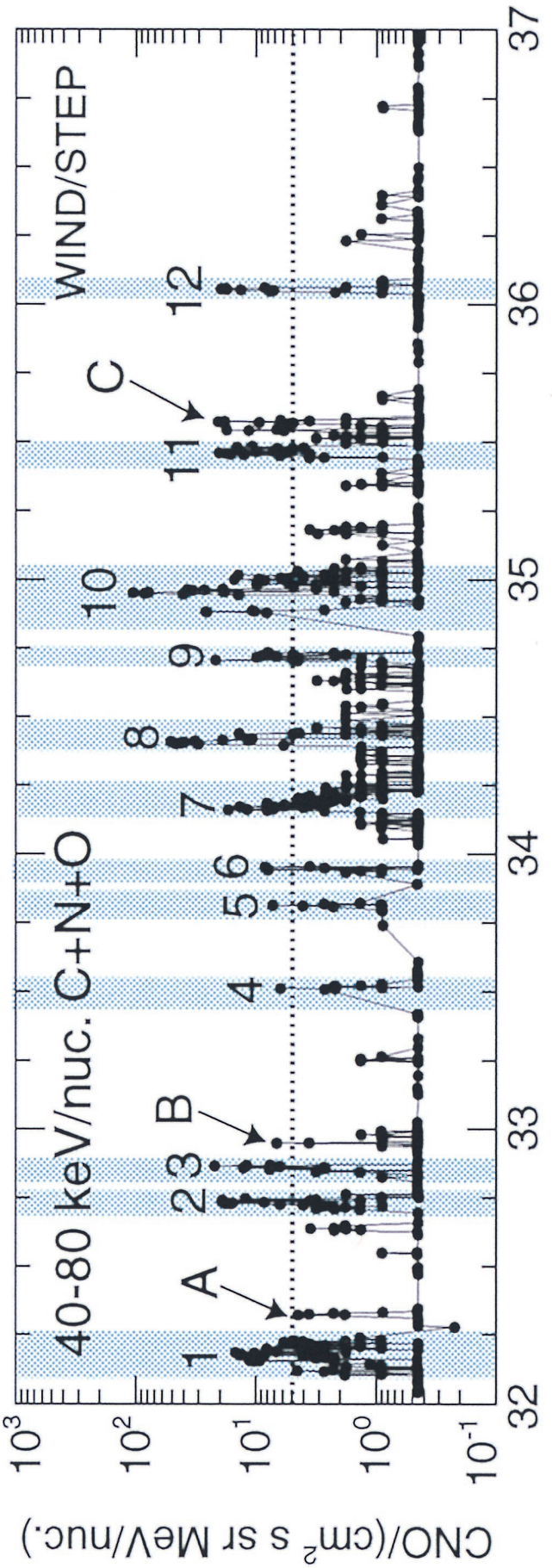


**Plate 1.** High time resolution (96 s) spin-averaged 40–80 keV/nucleon C + N + O intensity measured by STEP during a 5-day interval beginning on day 32, 1995. The dashed horizontal line denotes the minimum threshold required by an enhancement in the CNO intensity to be identified as an upstream event. The numbers 1–12 and the shaded vertical bands highlight the 12 upstream events selected during this period.

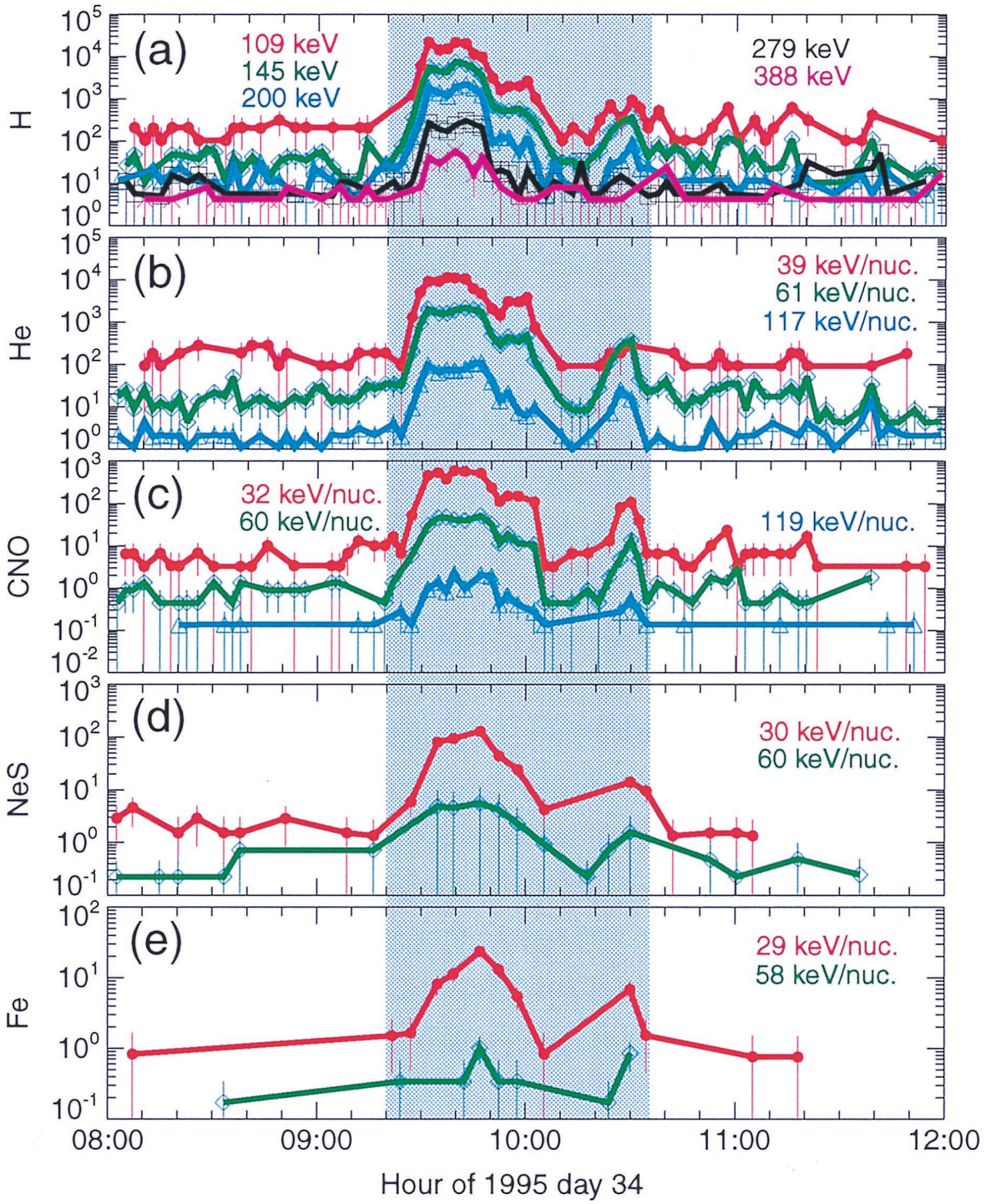


**Plate 2.** Ninety-six second spin averages of (a) H, (b) He, (c) CNO, (d) NeS, and (e) Fe intensities measured by STEP from 0800 to 1200 UT on day 34, 1995. The protons are measured in the 100–450 keV energy range while the other species are measured in the 30–160 keV/nucleon energy range. The shaded vertical band highlights the time interval (0920–1035 UT) corresponding to event 8 in Plate 1. The units of intensity are particles $(cm^2\ s\ sr\ MeV/nucleon)^{-1}$.

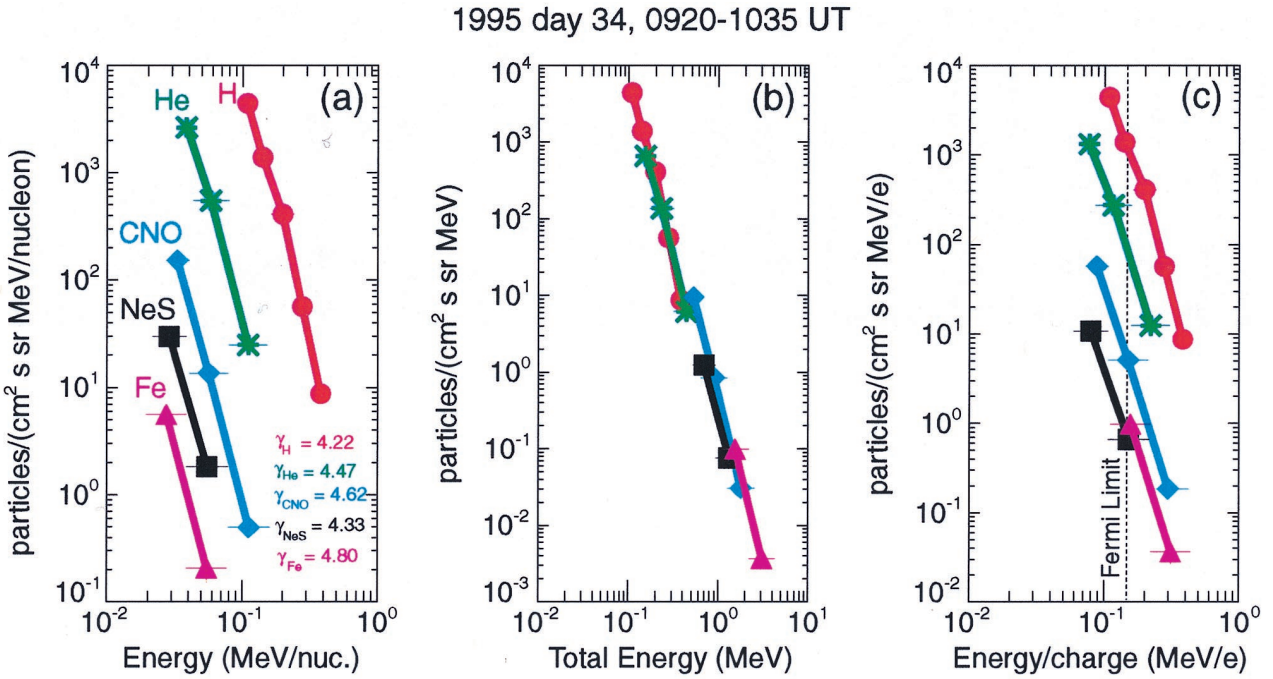


**Plate 3.** Differential energy spectra for all species measured from 0920 to 1035 UT on day 34, 1995 (event 8 in Plate 1) plotted versus (a) energy/nucleon, (b) total energy, and (c) energy/charge (assuming solar wind charge states). The unit of energy is MeV. The quantity $\gamma$ in Plate 3a is the power law spectral index, and the associated subscript denotes the species. The uncertainties in the values of $\gamma$ are $\leq$30%. The dashed vertical line in Plate 3c is drawn at 150 keV/*e* to identify the predicted upper limit of the Fermi acceleration process [*Lee*, 1982].

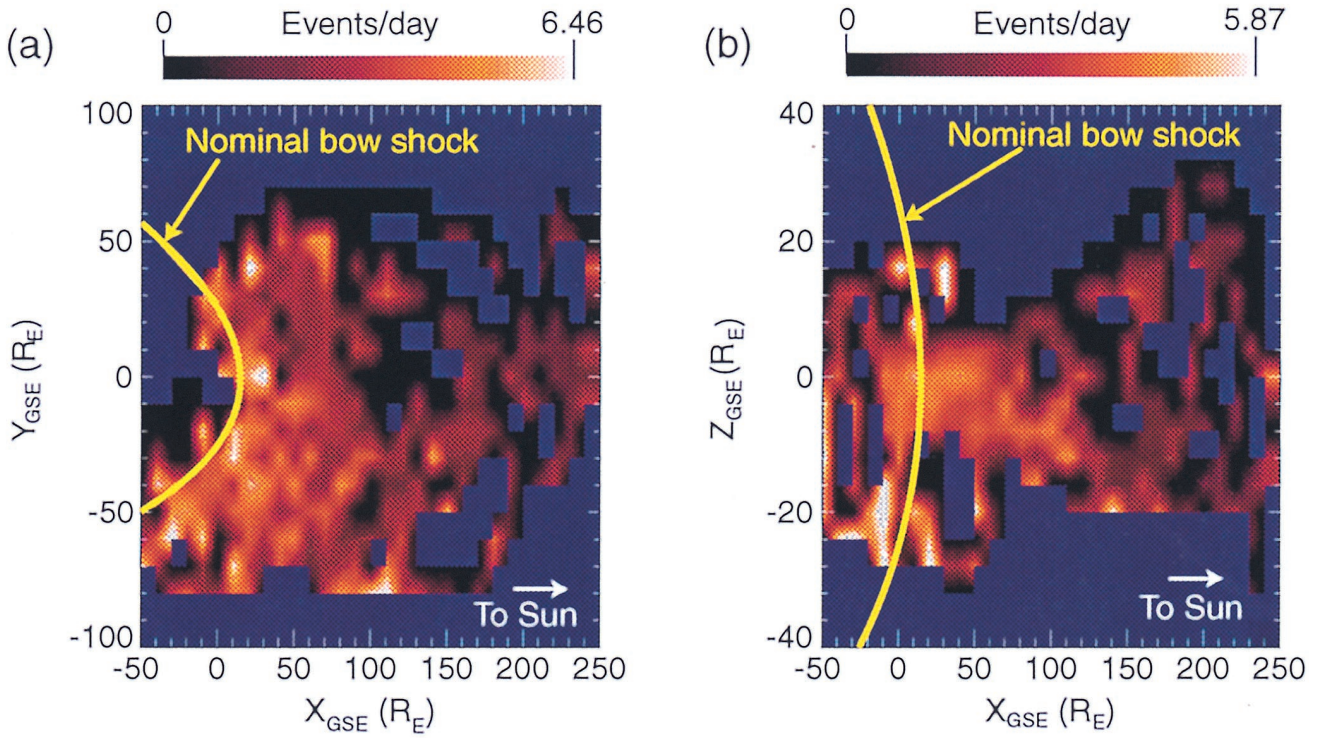


**Plate 4.** Spatial occurrence rate of upstream events normalized to the number of observation days projected in (a) the *XY* plane and (b) the *XZ* plane. The brightest regions correspond to the highest number of events detected per observation day (see the color bars above the panels). Blue regions identify locations where Wind did not make any measurements. Yellow curves show the nominal location of the bow shock, as defined by a paraboloid with equation $43.5X = 630 - Y^2 - Z^2$ [*Ipavich et al.*, 1981a].

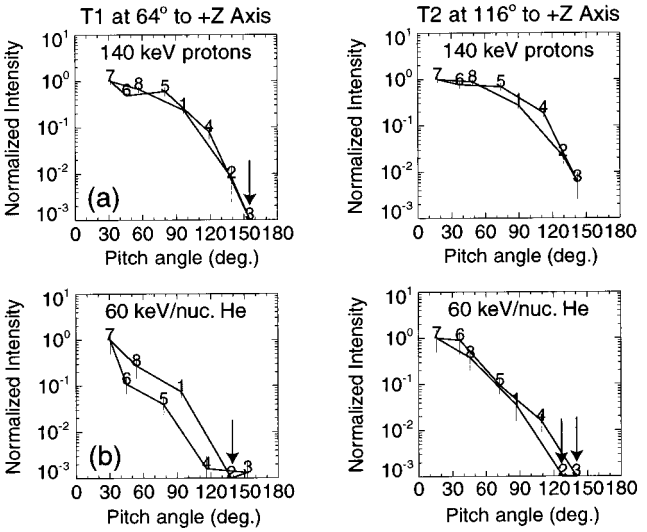


**Figure 2.** Pitch angle distributions of (a) 120–160 keV protons, and (b) 40–80 keV/nucleon He ions measured in the solar wind frame in T1 and T2 (see Figure 1) from 0920 to 1030 UT on day 34, 1995 (event 8 in Plate 1). For each telescope, the intensity measured in each sector is normalized to the maximum intensity during the interval, and plotted versus the pitch angle. The numbers 1–8 refer to the intensities measured in the corresponding sectors of T1 and T2, and the arrows identify sectors that measured zero counts (although plotted at $10^{-3}$) during the interval.

lyzed here), *Mason et al*. [1996] and *Dwyer et al*. [1997] had reported that the events were associated with a preexisting population of energetic particles accelerated in CIRs or SEPs, respectively. Thus, to obtain reliable spectral and composition information for the upstream events it is necessary to eliminate the possible contribution of all independent interplanetary populations.

The energy spectra for each species during all the events were derived by subtracting the corresponding "interplanetary backgrounds" from the mean intensities measured during the events. Plate 3 shows the interplanetary background corrected differential energy spectra for all species for event 8 plotted versus energy/nucleon, total energy, and energy/charge. The interplanetary background spectrum is derived from the mean intensities measured during 75-min intervals, i.e., the same interval as the event duration time, before and after the event (see Plate 2). Only data with uncertainty $\leq 30\%$ are included in these and all the spectra analyzed here.

The charge states assumed for each species in Plate 3c are the mean ionization states corresponding to a temperature of $1.2 \times 10^6$ K [*Arnaud and Rothenflug*, 1985] and are indicative of those measured typically in the fast solar wind [*von Steiger et al*., 1997]. These are $He^{2+}$, $CNO^{6+}$, $NeS^{8.68+}$, and $Fe^{9.84+}$. Since the charge states of heavier ions do vary from one potential source of these upstream ions to another, our assumed charge states do have inherent uncertainties. We note that the largest uncertainty occurs for the CNO spectrum if it is dominated by ions of ionospheric origin, i.e., by $O^+$. In this case, the CNO intensity in Plate 3c would be lower by a factor of 6 and the energy/charge would be higher a factor of 6. However, measurements of $O^+$ ions in the upstream region show that $O^+$ events are rare when compared with the actual occurrence rate of the upstream events [*Möbius et al*., 1986; *Christon et al*., 1999]. In addition, since the presence of NeS and Fe (see Plate 2) indicates a solar origin for these events, the typical uncertainties in the heavier ion spectra should be less than a factor of 2 even if the ions were in different charge states than what we have assumed. Further support for the above arguments may be obtained from the measured abundance ratios discussed in section 4.4 and the fact that most of the events were observed when the solar wind speed at Wind was greater than $\sim$450 km $s^{-1}$, as shown in section 5.3.

Plate 3a shows that the energy spectra between 30 and 300 keV/nucleon of all species obey power laws with spectral index $\gamma \sim 4.5$. From Plate 3b we note that the proton and He contributions to the total energy ion spectrum between 0.1 and 0.5 MeV are comparable, while the spectrum above $\sim$0.5 MeV is dominated by the heavier ions. Plate 3c shows that the energy spectra of all species extend above $\sim$150 keV/$e$. We remark that a typical feature of the upstream events studied here was that the total energy ion spectrum above $\sim$0.5 MeV is dominated by heavier ions and that this result is not affected by the instrumental energy range because STEP can measure protons up to $\sim$2.5 MeV and He ions up to $\sim$5.12 MeV in total energy. However, since the lower-energy threshold of STEP is $\sim$30 keV/nucleon, we cannot determine the heavy ion contribution to the total energy ion spectrum between 0.1 and 0.5 MeV.

### 4.4. Composition

Figure 3 shows the mass distribution of the heavy ions (mass $M > 8$) in the 40–200 keV/nucleon energy range detected during the 12 upstream events shown in Plate 1 (with the interplanetary background subtracted). The interplanetary background for these 12 events is determined from the corresponding preevent and postevent time intervals defined in section 4.3. The clear peaks around $M = 12$ and $M = 16$ correspond to C and O, respectively, while the relatively broader peaks from $M = 20$–35 and $M = 50$–65 correspond to species over the Ne-S range and the Fe group, respectively. We obtain the various ion abundances relative to O from the relative heights of the histogram around their respective masses (e.g., $M = 15$–17 for O) by taking account of their detection efficiencies relative to O in the 40–200 keV/nucleon

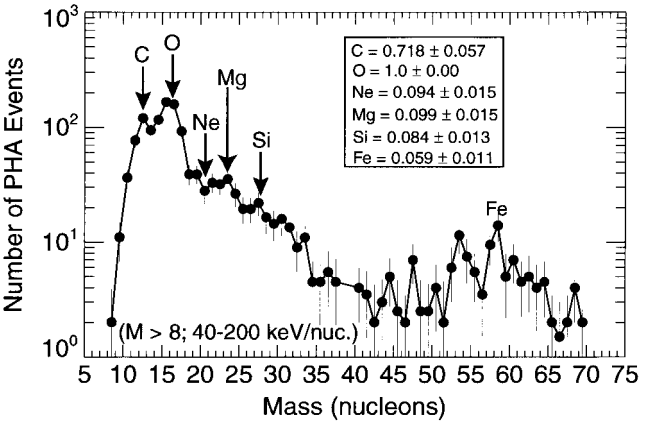


**Figure 3.** Mass distribution of the heavy ions (mass $M > 8$) in the 40–200 keV/nucleon energy range detected during the 12 upstream events shown in Plate 1. This histogram has had the interplanetary background (see text) subtracted from it. The mean abundances of various heavy ions relative to O for the 12 events are also given.

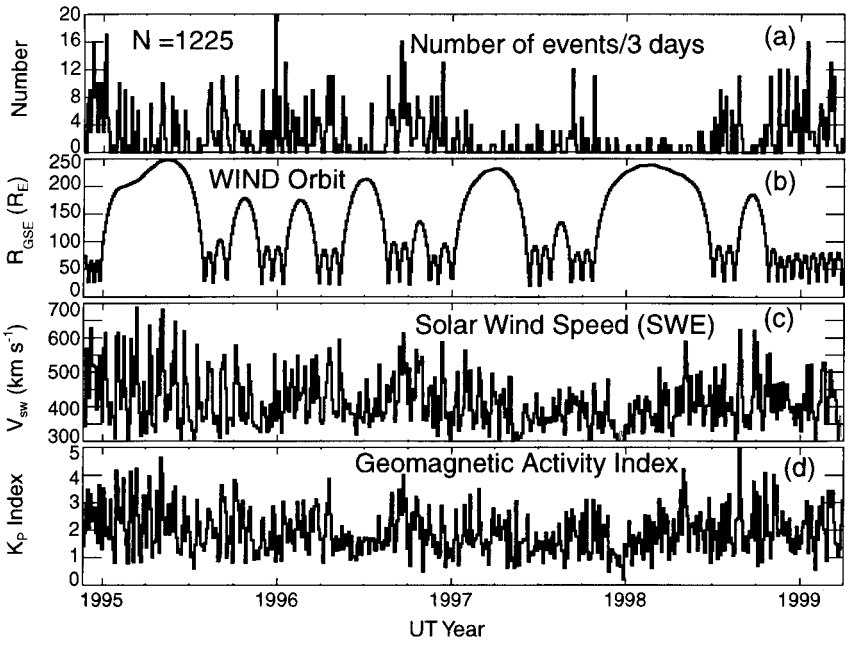


**Figure 4.** Three-day averages of (a) the occurrence rate of upstream events, (b) the radial distance of WIND in $R_E$, (c) the solar wind speed $V_{sw}$ in km s$^{-1}$ measured by the Solar Wind Plasma Experiment (SWE) [*Ogilvie et al*., 1995], and (d) the geomagnetic activity index $K_p$ obtained from www.ngdc.noaa.gov:80/stp/geomag/ from 1994 day 325 to 1999 day 92.

energy range. The He/O ratio for these 12 events was = 79.48 ± 14.17. The heavier ion abundances are given in Figure 3 and are typical of those measured during the upstream events analyzed in this paper.

## 5. Conditions of Upstream Event Observation

### 5.1. Overview and Long-Term Trends

Figure 4 provides an overview of our observations from 1994 day 325 to 1999 day 92. Figure 4 shows 3-day averages of the occurrence rate of upstream events, the radial distance of WIND in $R_E$, the solar wind speed $V_{sw}$ in km s$^{-1}$, and the geomagnetic activity index, $K_P$. Figure 4 shows that with the exception of a 60-day interval starting from about day 180 1997, the event occurrence rate from the beginning of 1997 until the middle of 1998 was substantially lower when compared with that observed from late 1994 to 1997 and also from the middle of 1998 until 1999 day 92. It is also clear from the figure that the event occurrence rate increased when Wind was close ($\lesssim$150 $R_E$) to the Earth, as may be seen during the relatively quieter period of 1997 until the middle of 1998 in Figures 4a and 4b. Finally, we note that there is a close correspondence between the event rate and enhancements in both $V_{sw}$ and $K_p$.

### 5.2. Spatial Occurrence Rate of the Events

Plate 4 shows the spatial occurrence rate of the events normalized to the number of observation days projected in the XY, and the XZ plane. These data are obtained by dividing the number of events observed in each $10 \times 10\ R_E$ region of $XY$ space and $10 \times 4\ R_E$ region of $XZ$ space by the number of days that Wind actually spent in that region. Blue regions identify locations where Wind did not make any measurements. We note that (1) upstream events were observed at all locations within $\pm 80\ R_E$ in $Y_{GSE}$, (2) the greatest frequency of events occurred within $\sim 100\ R_E$ in $X_{GSE}$ although the ions are observed up to the libration point, and (3) the frequency of events was generally higher when $|Z_{GSE}| < 20\ R_E$. We also remark that (1) the event rate in the dawn-noon sector was 1.45 compared with 0.63 in the noon-dusk sector, and (2) the event rate for $|Y_{GSE}| > 30\ R_E$ was 1.33 compared with 0.77 for $|Y_{GSE}| < 30\ R_E$.

### 5.3. Relationship Between the Event Occurrence Rate and $V_{sw}$ and $K_p$

The top panels in Figure 5 display the distribution of upstream events (solid circles) and the number of observation days (open circles) versus $V_{sw}$ (Figure 5a) and the $K_p$ index (Figure 5b) while the bottom panels show the daily occurrence rates of the events versus $V_{sw}$ and $K_p$. From the bottom panels of Figure 5 we note that (1) the event rate increases with both $V_{sw}$ and $K_p$, and (2) the probability of observing more than 1 event per day increases when $V_{sw} > 450$ km s$^{-1}$ and/or $K_p > 2$. Recently, *Baker et al*. [1994] have reported that the arrival of high-speed streams at Earth tends to energize the magnetosphere, which indicates that $V_{sw}$ and $K_p$ are themselves related to each other. Thus it appears that the correlations shown in Figure 5 are also somehow dependent on each other.

### 5.4. IMF Orientation and Linear Miss-Distance

In the Fermi process, ions are accelerated most efficiently near the quasi-parallel portions of the bow shock where the angle $\theta_{Bn}$ between the interplanetary magnetic field (IMF) and the shock normal $\lesssim 45°$ [*Ellison et al*., 1990]. Thus, for a radial IMF, the Fermi process should be most efficient near the nose of the bow shock, while for a nominal IMF ($\sim 45°$ to the radial direction) the process should be most efficient near the dawn-noon portions. In contrast, in the magnetospheric leakage model, the majority of the ion events should occur in

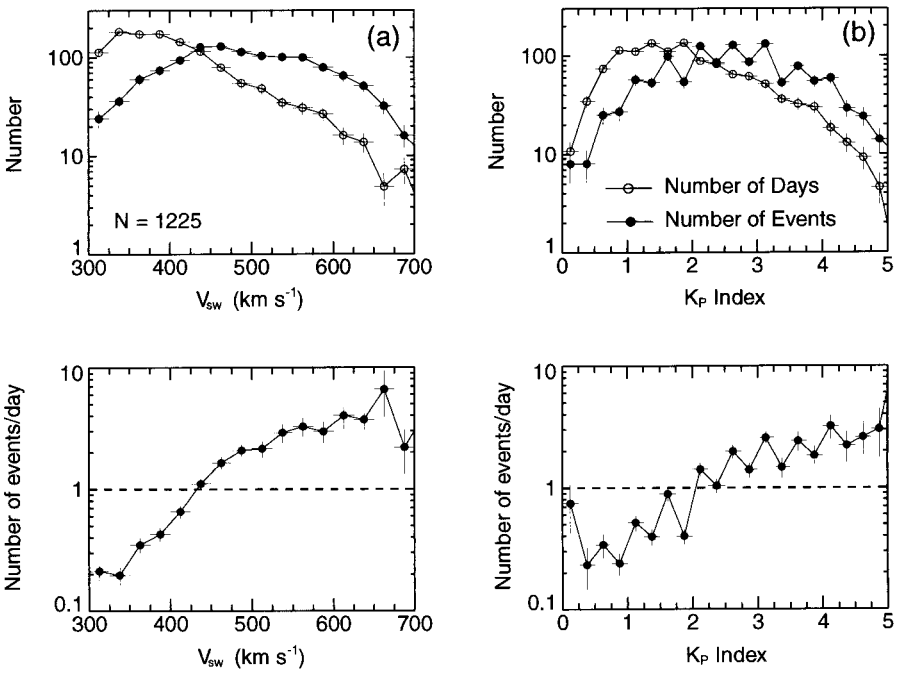


**Figure 5.** Distribution of upstream events (solid circles) and the number of observation days (open circles) versus (a) $V_{sw}$ and (b) $K_p$. The lower panels show the daily occurrence rates of the events versus $V_{sw}$ and $K_p$.

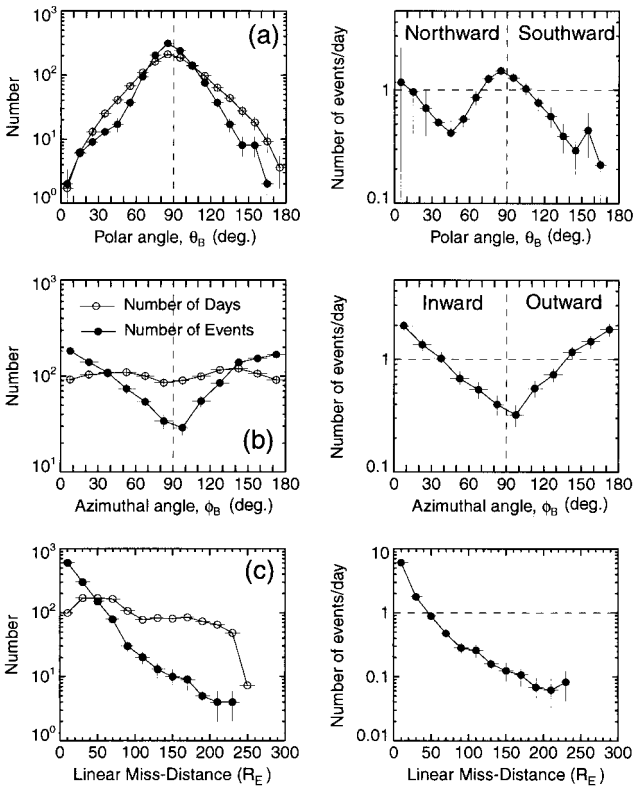


**Figure 6.** Same as Figure 5 but versus (a) the IMF polar angle $\theta_B$, (b) the IMF azimuthal angle $\phi_B$, and (c) the linear miss-distance $D_M$ in $R_E$ (see text for definition). Note that the value of $\phi_B$ has been modified to discern the sector polarity of the IMF (see text).

the noon-dusk sector when particles accelerated in the plasma sheet during periods of geomagnetic activity escape into the upstream region [*Sibeck and McEintire*, 1988]. Geomagnetic activity, in turn, is most intense when the IMF has a southward component. In addition, both models also require that the IMF lines passing through the spacecraft should be connected to the source region.

To test the above mentioned predictions of both models, we have surveyed the IMF orientation relative to Wind and the bow shock during the events. Because the IMF components can fluctuate dramatically during the course of an event, a statistical study of its orientation averaged over the duration of many events will yield erroneous results. Therefore, for each event we obtain the IMF polar angle $\theta_B$ and azimuthal angle $\phi_B$ averaged during the 10-min interval for which the 60 keV/nucleon CNO intensity reached a peak. In the GSE coordinate system, $\theta_B$ is measured from the $+Z$ axis and $\phi_B$ is measured from the $+X$ axis in the $XY$ plane.

For additional confirmation that these events do indeed originate from the Earth, we have computed the linear miss-distance, $D_M$, for each event. Here $D_M$ is measured in $R_E$, and is defined as the minimum distance (during the event) that a straight line extended along the locally measured magnetic field vector misses an intersection with the Earth. *Stansberry et al.* [1988] had reported that owing to extensive field line meandering between the Earth and spacecraft located beyond $\sim$150 $R_E$ upstream, the local IMF orientation is generally not reliable in determining whether the spacecraft is magnetically connected to the bow shock or not. Thus, even though this effect could yield unusually large values for $D_M$ when Wind was far upstream, in general, if $D_M < 40\ R_E$, then there is a reasonable possibility that the magnetic field lines passing

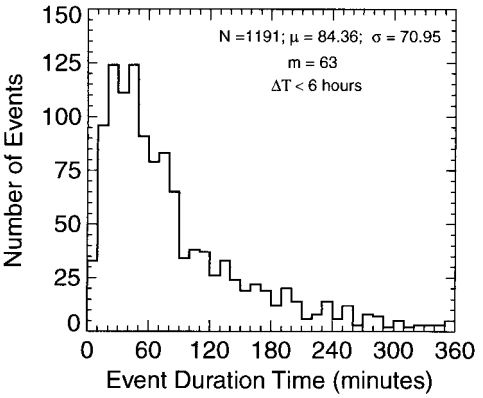


**Figure 7.** Distribution of the event duration times (in minutes) of $N = 1191$ events. The quantities $\mu$, $\sigma$, and $m$, respectively, denote the mean, the standard deviation, and the median of the distribution. Only events with duration times $\Delta T < 6$ hours (see text) are included in the statistical summary.

through Wind probably intersected the bow shock during the event.

Figure 6 shows the distribution of upstream events (solid circles) and the number of observation days (open circles) plotted versus $\theta_B$, $\phi_B$, and $D_M$. To discern the sector polarity of the IMF, we have modified the value of the azimuthal angle for $\phi_B > 180°$ to $\phi_B = 360 - \phi_B$. This ensures that if $\phi_B < 90°$ then the IMF has an inward sector, whereas if $\phi_B > 90°$, then the IMF has an outward sector. The right-hand panels show the daily occurrence rates of the events versus $\theta_B$, $\phi_B$, and $D_M$. We note that (1) 909 events ($\approx$74%) were observed when the IMF was within 20° of the ecliptic plane, (2) 892 events ($\approx$73%) were observed when the IMF was within 45° of the radial direction, (3) there is no clear preference for the orientation and the sector polarity of the IMF, and (4) $D_M$ for 902 events ($\approx$74%) was $\leq 40\ R_E$, which emphasizes the importance of magnetic connection between Wind and the bow shock for observing upstream events. We remark that a survey of the statistical properties of $\theta_B$ and $\phi_B$ at 96-s resolution (not shown) during all the events yields similar results.

## 6. Characteristics of Upstream Events

### 6.1. Event Duration Times

Figure 7 shows the distribution of duration times for 1191 of the 1225 events in the survey. The remaining 34 events not included here had duration times $\Delta T > 6$ hours. The values of the mean $\mu$ and the median $m$ taken together with the peak of the distribution indicate that the majority of the events lasted $\lesssim$90 min, which was also typical of the 12 events shown in Plate 1. Many of the events that lasted $\gtrsim$90 minutes were in fact composed of several shorter duration events that occurred within $\lesssim$30 min of each other, as discussed in section 3.

### 6.2. Angular Distributions

To avoid averaging over fluctuations in the IMF occurring during the course of the events, we have obtained the pitch angle distributions in the solar wind frame for each event during the 10-min interval for which the 60 keV/nucleon CNO intensity reached a peak. We then identified the sectors of both T1 and T2 which measured the maximum CNO intensity during this 10-min interval. For example, in Figure 2 the maximum intensity for both H and He (and also for CNO) in T1 and T2 was observed in sector 7 at pitch angles of $\sim$30° and $\sim$15°, respectively. Hereinafter this quantity is referred to as the pitch angle $\alpha_M$ of the maximum sector.

Figure 8 shows histograms of $\alpha_M$ in T1 and T2 for all events. Only pitch angles with uncertainty $\leq$30% are included in this plot. Note that the two preferred values for $\alpha_M$ are $\sim$30° and $\sim$150°, implying that the majority of the ions during the events were traveling parallel and antiparallel, respectively to the IMF. Further analysis (not shown) has revealed that the maximum intensity during the events was measured in sectors 5–8 of T1 and T2, indicating that the dominant anisotropy was aligned along the magnetic field lines and away from the Earth. A close examination of the magnetic field data during events with $\alpha_M$ close to $\sim$90° has revealed that the IMF either pointed out of the ecliptic plane or was oriented at large angles to the radial direction.

### 6.3. Electron Association

We have also investigated whether the 3DP instrument on board Wind detected energetic (20–48 keV) electrons during the upstream events analyzed in this paper. We found that the intensity of 20–48 keV electrons was enhanced by at least an order of magnitude above the corresponding interplanetary background level during 307 of the 1225 ion events analyzed in this paper. A detailed comparison between the characteristics of events that were associated with electrons and those that were not is beyond the scope of this paper and is deferred to a later study.

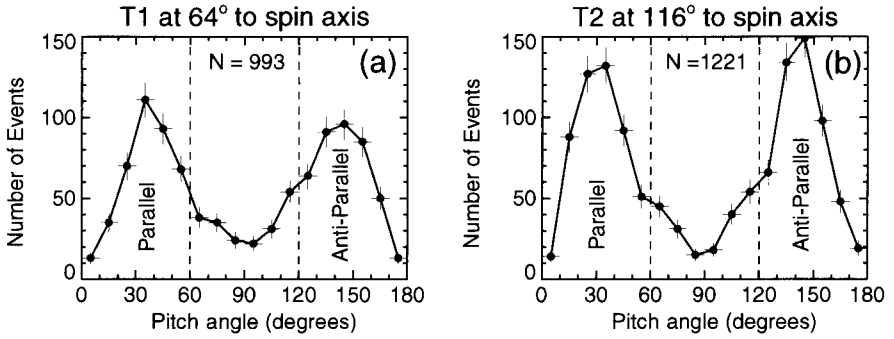


**Figure 8.** Histograms of the pitch angles of the sectors of (a) T1 and (b) T2 which detected the maximum intensity for $\sim$60 keV/nucleon CNO ions in the solar wind frame during the upstream events.

### 6.4. Energy Spectra

Figure 9 shows histograms of the spectral indices of He, CNO, NeS, and Fe, which were obtained from power law fits to the differential energy spectra like the ones shown in Plate 3a. This plot only includes indices with uncertainty ≤30%. The values of the median $m$ and the mean $\mu$ taken together with the fact that all the distributions peak between 4 and 5 indicate that most of the heavy ion ($M \geq 4$) spectra were softer than those measured typically in CIRs [*Mason et al*., 1997] or SEPs [*Reames*, 1999]. We remark that proton spectral indices (not shown) for 953 events exhibited a somewhat broader distribution when compared with those shown in Figure 9, with mean, standard deviation, and median of $\mu = 5.17$, $\sigma = 1.45$, and $m = 5.12$, respectively.

Plate 5 shows the relative number of upstream events versus the maximum energy observed for each ion type, during the events. The fraction of events is plotted versus energy/nucleon, total energy, and energy/charge. Table 1 shows the total number of events analyzed for each species and the fraction of events that were associated with appreciable intensity enhancements above several representative energies. From Table 1 and Plate 5 we note that (1) the number of events with He, CNO, NeS, and Fe intensity enhancements above ~0.5 MeV is more than a factor of 3 greater than the corresponding number of events with proton enhancements, (2) the proton spectrum did not extend above ~0.5 MeV during ~84% of the events, and (3) intensity enhancements above ~150 keV/e for all species were detected in ≳40% of the events. Furthermore, we found that most of the proton spectra that extended above ~300 keV and ~30% of the He and CNO spectra above ~80 keV/nucleon softened at higher energies, indicative perhaps of an exponential-like roll-over. Similar spectral forms for protons and helium were also observed by *Ipavich et al*. [1981a], although the roll-over occurred at significantly lower energies (~65 keV/charge) than reported here.

### 6.5. Composition Analysis

In order to survey the ion composition in upstream events and also to investigate their evolution during the course of the Wind mission, we have divided the data set into 5 periods, namely (1) 1994 (from day 325) and 1995, (2) 1996, (3) 1997, (4) 1998, and (5) 1999 (until day 92). Plate 6 shows the background subtracted mass histograms of the heavy ions ($M > 8$) in the 40–200 keV/nucleon energy range detected during all the upstream events observed during each of the five periods. Note that the histogram for 12 events in 1995 shown in Figure 3 is similar to the one obtained for all the events observed during 1995 (shown in red in Plate 6).

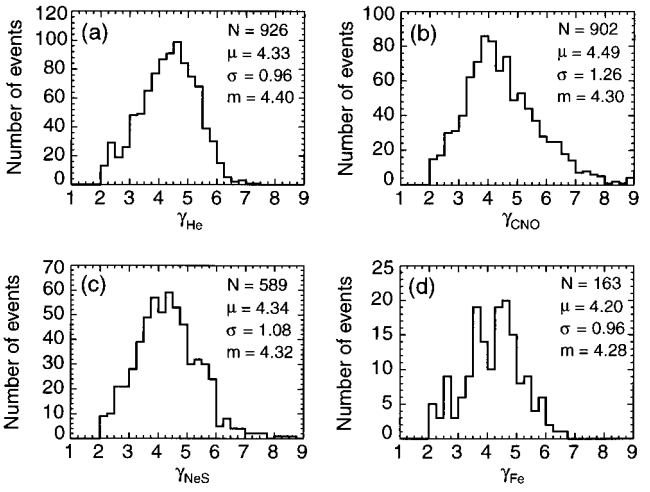


**Figure 9.** Histograms of the differential energy power law spectral indices of (a) He, (b) CNO, (c) NeS, and (d) Fe measured in the upstream events.

**Table 1.** Relative Number of Upstream Events With Intensity Enhancements Above a Given Total Energy $E$

| Species | Number | $E > 0.15$ | $E > 0.3$ | $E > 0.5$ | $E > 1.0$ | $E > 2.0$ |
|---|---|---|---|---|---|---|
| H | 1076 | 87.8% | 37.0% | 16.2% | 4.5% | 1.5% |
| He | 1048 | 86.6% | 84.6% | 60.1% | 20.8% | 4.5% |
| CNO | 990 | 80.8% | 80.8% | 80.8% | 70.9% | 33.4% |
| NeS | 820 | 66.9% | 66.9% | 66.9% | 46.9% | 26.2% |
| Fe | 593 | 48.4% | 48.4% | 48.4% | 48.4% | 31.4% |

Total energy $E$ in MeV.

The average ion abundances relative to O for each period and also for all upstream events are obtained using the method described in section 4.4. Table 2 provides the mean composition ratios for all the upstream events. Notice the similarity between these values and those obtained for just 12 events in 1995, as listed in Figure 3. The solar wind abundances given in the table are the "in-ecliptic" and "coronal hole" values [*von Steiger et al*., 1997], which are indicative of typical abundances in the slow- (~300–450 km $s^{-1}$) and the fast- (~600–750 km $s^{-1}$) solar wind, respectively. Table 2 also lists the abundances measured in CIRs [*Mason et al*., 1997] and SEPs [*Reames*, 1999], and those measured in the Earth's magnetosheath, plasma sheet, and ring current during periods of geomagnetic activity [*Gloeckler and Hamilton*, 1987].

Plate 7 shows the ion abundances in upstream events for each of the five long-term periods. We note from Table 2 and Plate 7 that the ion composition in upstream events is, in general, similar to that measured typically in the solar wind. Specifically, we note that (1) the He/O ratio drops significantly during 1997, (2) the C, Ne, Mg, and Si abundances relative to O remain relatively steady (within ~30%) during all five periods, and (3) the Fe/O ratio remains relatively constant during the first four periods, but increases by almost a factor of 3 during 1999.

## 7. Discussion

### 7.1. Conditions of Upstream Event Observation and Their Implications

We have investigated the temporal and spatial occurrence rates, and the solar wind and magnetospheric conditions for 1225 upstream events observed by EPACT/STEP from 1994 day 325 to 1999 day 92. Our results show the following:

1. The event occurrence rate decreased dramatically to <1 event per day during 1997 and early 1998; the occurrence rate was higher when both $V_{sw}$ and $K_p$ were enhanced, i.e., when $V_{sw} > 450$ km $s^{-1}$ and $K_p > 2$.
2. Most events were observed within $\pm 80\, R_E$ in $Y_{GSE}$ and inside ~100 $R_E$ in $X_{GSE}$, although the events occurred at all locations of the Wind orbit.
3. About ~73% of the events were observed when the IMF was close to the ecliptic plane and pointed along the radial direction; there was no clear preference for the sector polarity and the orientation of the IMF.

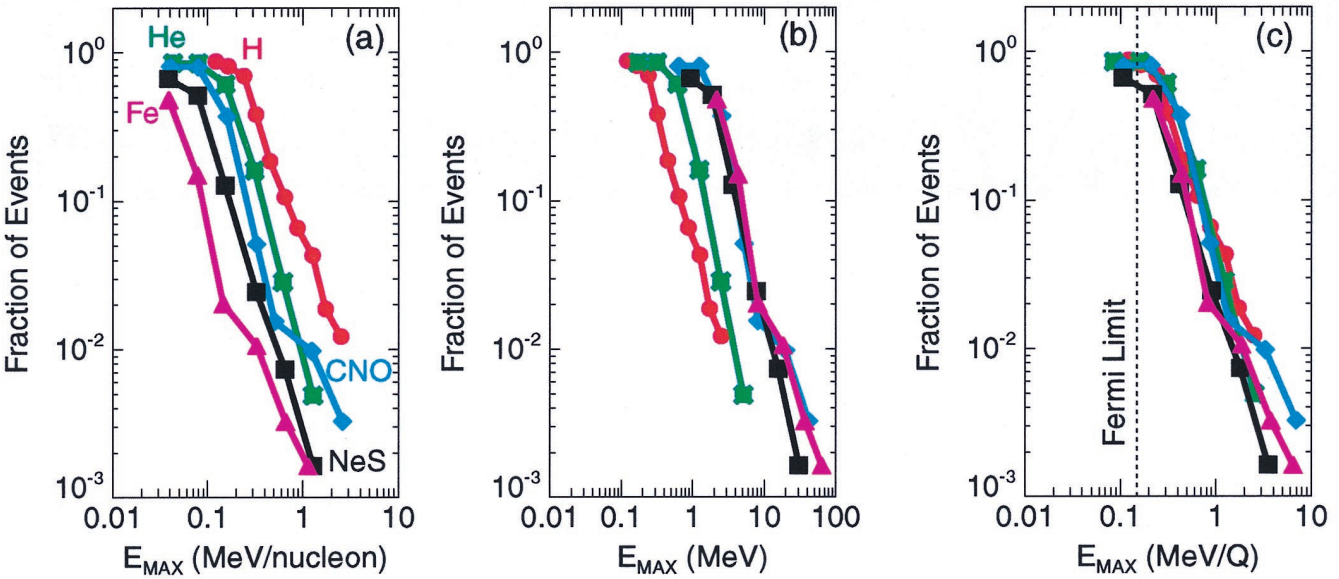


**Plate 5.** Relative number of upstream events (normalized to $N = 1225$) versus the maximum energy observed for each ion type, during the events. The fraction of events is plotted versus (a) energy/nucleon, (b) total energy, and (c) energy/charge. The dashed vertical line at 150 keV/*e* in Plate 5c may be used to estimate the relative number of events with intensity enhancements above the Fermi limit [*Lee*, 1982] for any species.

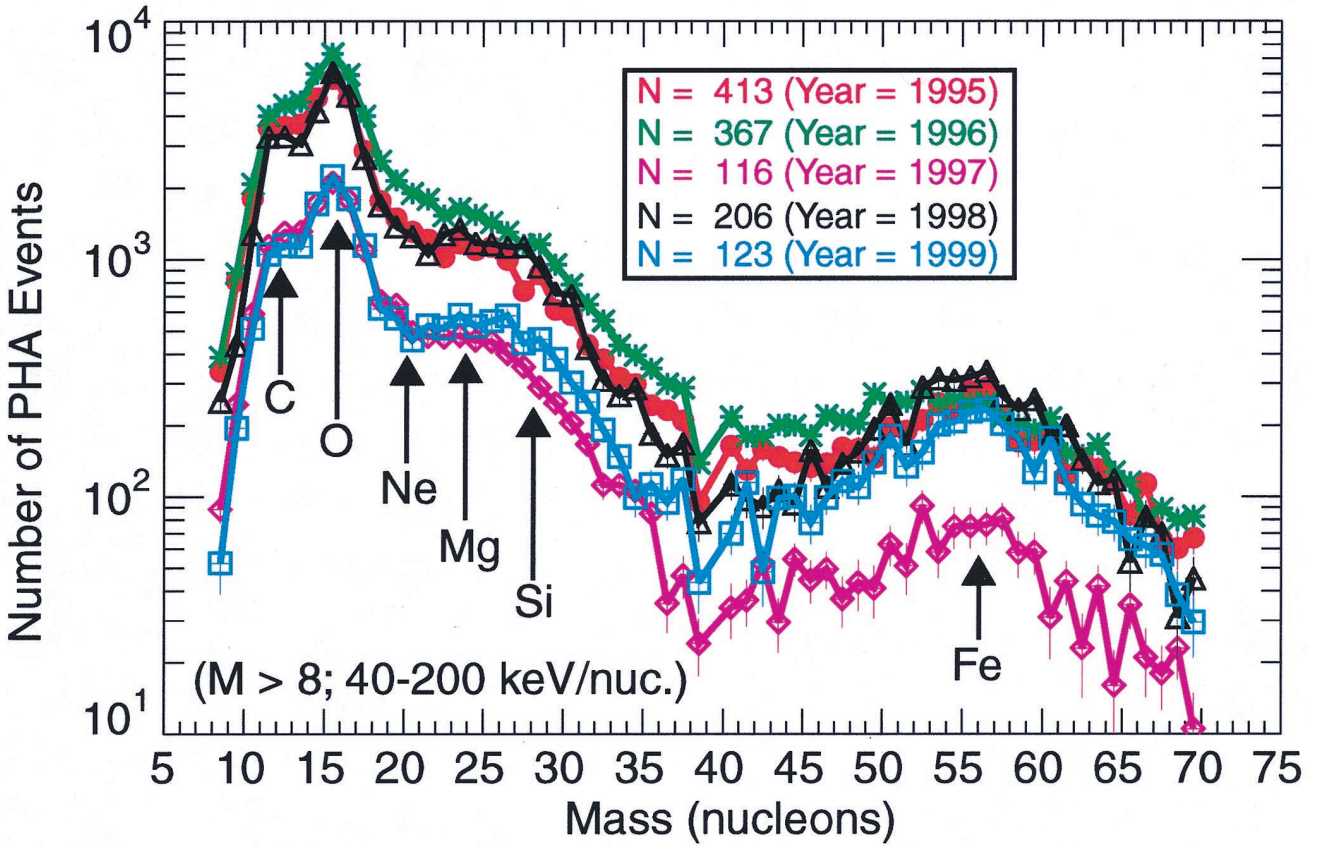


**Plate 6.** Same as Figure 3 but for the upstream events observed during the five long-term periods defined in the text. The quantity $N$ denotes the number of events observed during the corresponding period. The histogram for 1995 also includes data for the events observed from 1994 day 325 to 1995 day 1.

**Table 2.** Heavy Ion Abundances in Upstream Events

| Element | Upstream Events ($N$ = 1225) | Fast SW* | Slow SW* | CIRs† | SEPs‡ | Magneto Sheath‡ (Disturbed) | Plasma Sheet§ (Substorm) | Ring Current§ (Storm) |
|---|---|---|---|---|---|---|---|---|
| He | 104 ± 2.43 | 83 ± 25 | 75 ± 20 | 113 ± 20 | 57 ± 3 | 31 | 0.18 | 0.1 |
| C | 0.751 ± 0.006 | 0.7 ± 0.1 | 0.72 ± 0.1 | 0.75 ± 0.12 | 0.47 ± 0.01 | ··· | ··· | ··· |
| O | ≡1 | ≡1 | ≡1 | ≡1 | ≡1 | ≡1 | ≡1 | ≡1 |
| Ne | 0.118 ± 0.002 | 0.14 ± 0.01 | 0.14 ± 0.02 | 0.21 ± 0.05 | 0.15 ± 0.01 | ··· | ··· | ··· |
| Mg | 0.116 ± 0.002 | 0.08 ± 0.02 | 0.16 ± 0.02 | 0.13 ± 0.03 | 0.20 ± 0.01 | ··· | ··· | ··· |
| Si | 0.121 ± 0.002 | 0.05 ± 0.01 | 0.19 ± 0.01 | 0.11 ± 0.02 | 0.15 ± 0.01 | ··· | ··· | ··· |
| Fe | 0.063 ± 0.001 | 0.06 ± 0.01 | 0.12 ± 0.01 | 0.08 ± 0.03 | 0.13 ± 0.01 | ··· | ··· | ··· |

*From *von Steiger et al*. [1997].
†From *Mason et al*. [1997].
‡From *Reames* [1999].
§From number density ratios measured by *Gloeckler and Hamilton* [1987].

4. Most events were observed when the spacecraft was most likely magnetically connected to the bow shock ($D_M \lesssim 40\ R_E$).

Point 1 may be explained as follows: *Baker et al*. [1994] have shown that the arrival of high-speed streams at ~1 AU tends to trigger geomagnetic activity. Recently, *Sanderson et al*. [1998] have reported that the appearance of high-speed streams at Wind from launch till May 1997 was influenced by the latitudinal separation between Wind and the heliospheric current sheet (HCS) at ~1 AU; a sufficiently large separation enabled the spacecraft to move out of the slow-speed flow of the streamer belt that straddled the HCS and sample high-speed streams that emanated from polar coronal holes. In addition, *Sanderson et al*. [1998] also showed that the angular separation between WIND and the HCS was substantially greater during the relatively active solar periods of 1994 and 1995 when compared with the quieter period of 1997. On the basis of these results we suggest that regardless of their origin, the occurrence rate of upstream events is also ultimately related to the phase of the solar cycle.

Since the event rate correlates with both $V_{sw}$ and $K_p$, i.e., quantities that are themselves related to each other [*Baker et al*., 1994], we suggest that a correlation between any characteristic of the events and either quantity cannot be used to argue for or against the two popular models. However, we note that a positive correlation between the ion intensity in upstream events and $K_p$ has often been used as evidence in support of magnetospheric leakage [e.g., *Anagnostopoulos*, 1998]. Similarly, one could also argue that higher $V_{sw}$ results in a stronger compression at the bow shock, which in turn increases its acceleration efficiency and produces more upstream events [e.g., *Ellison et al*., 1990]. The subjective nature of these arguments was confirmed when we found that the spectral indices for each species shown in Figure 9 anticorrelated with both $V_{sw}$ and $K_p$ with similar values (between 0.2 and 0.4) for the linear correlation coefficients. This indicates that the correlations with both quantities are of equal statistical significance and therefore provide little discriminatory evidence regarding the origin of the events.

Our analysis showed that the majority of the events occurred in the dawn-noon sector under a radial IMF (point 3) with a small miss-distance (point 4), indicating that the ions are observed predominantly near the quasi-parallel portions of the bow shock. This is consistent with the results of both *Scholer et al*. [1980] and *Mitchell and Roelof* [1983] and could simply be due to the Fermi process being more efficient where $\theta_{Bn} \lesssim 45°$ [*Jones and Ellison*, 1991]. However, our results also showed that the events were observed at all locations within $\pm 80\ R_E$ in $Y_{GSE}$ (point 2), with 672 events occurring at a rate of 1.33 for $|Y_{GSE}| > 30\ R_E$. A radial IMF for these events implies that the ions probably originated from all portions of the bow shock including the flanks where the shock is essentially quasi-perpendicular, rather than exclusively from the quasi-parallel part as predicted by the Fermi model [e.g., *Ellison et al*., 1990].

Conversely, a radial IMF and a small miss-distance for the events observed in the dawn-noon sector (an event rate of 1.45 represents 793 events) implies that the majority of the ions probably originated from the dawnside, which poses a problem for the magnetospheric model wherein ions escape predominantly from the dusk magnetpause [*Sibeck and McEntire*, 1988]. Thus the leakage model must explain how ions that leak from the duskside get transported in the upstream region across the predominantly radial IMF and get observed in the dawn-noon sector and still exhibit a strong field-aligned sunward anisotropy.

The above properties are consistent with the recent results of *Sanderson et al*. [1996], *Haggerty et al*. [1999], and *Dwyer et al*. [1999]. The former group reported the observation of upstream events by the 3DP instrument at all portions of the Wind orbit, while the two latter groups reported the simultaneous appearance (within a few minutes) of upstream ions at Wind and ACE at times when the separation in $Y_{GSE}$ and $Z_{GSE}$ between the spacecraft was $\gtrsim 50\ R_E$. Both, *Haggerty et al*. [1999] and *Dwyer et al*. [1999] have suggested that since during the simultaneous events the two spacecraft were likely to have been connected to different portions of the bow shock, the size of the source region was probably comparable to the entire size of bow shock, which poses a problem for both models.

### 7.2. Characteristics of Upstream Events and Their Implications

Our results for the event durations, electron association and the energy spectra, anisotropy, and composition of 0.03–2 MeV/nucleon ions during the 1225 events are the following:

1. The events typically lasted between 10 min up to 3 hours.
2. The angular distributions exhibited a strong field-aligned flow away from the Earth.
3. At least ~25% of the events were accompanied by ~35 keV electrons.
4. The energy spectra of 100–300 keV protons and 30–300

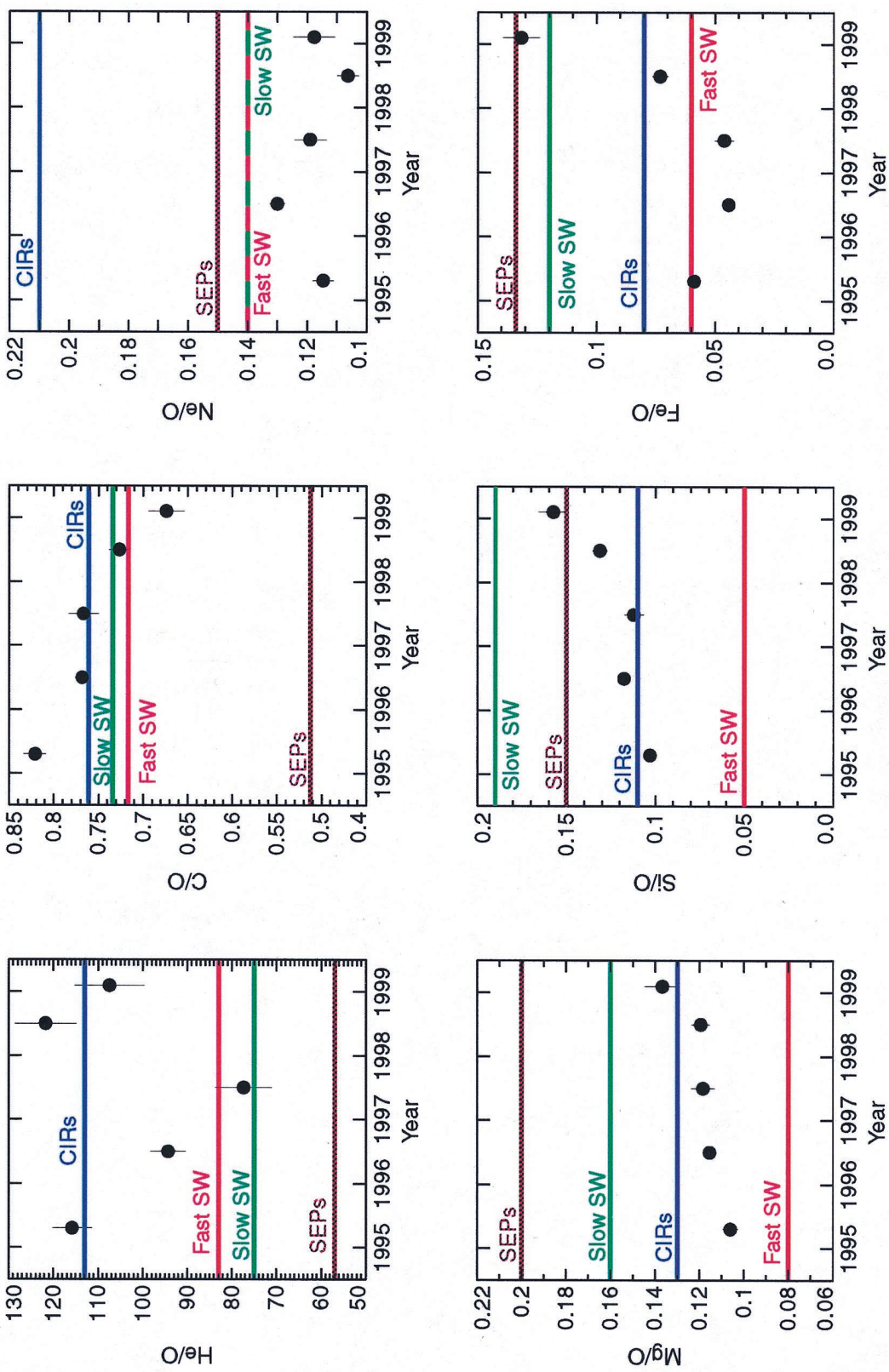


**Plate 7.** Heavy ion abundances relative to O measured in upstream events as a function of time. The abundance ratios for each period are plotted at the middle of the interval. The horizontal lines in each panel show the corresponding ratios measured in the fast (red) and slow (green) solar wind, in CIRs (blue), and in SEPs (brown) from Table 2.

keV/nucleon He, CNO, NeS, and Fe during ~70% of the events obeyed power laws with $\gamma$ between 3 and 5, while the energy spectra of He and CNO for ~30% of the events softened above ~80 keV/nucleon.

5. The number of events with enhancements in the He, CNO, NeS, and Fe intensities above ~0.5 MeV total energy is more than a factor of 3 greater than the corresponding number of events with proton enhancements.

6. The proton spectrum did not extend above ~0.5 MeV during ~84% of the events.

7. More than 75% of the proton He and CNO spectra, and $\gtrsim$40% of the NeS and Fe spectra extended above ~150 keV/$e$.

8. The ion composition in the events was similar to typical solar wind values.

Points 1 and 2, i.e., the average event duration of ~1–2 hours and the strong sunward field-aligned flow, are consistent with previous observations of upstream events [e.g., *Sanderson et al*., 1981], although these earlier results were based mainly on proton and He measurements. However, the remainder of our results (points 3–8) not only have important implications for some of the earlier results that were construed as strong evidence in support of the magnetospheric leakage model but also place new requirements and constraints on the source of the upstream ion populations.

It is presently accepted that if the total energy ion spectrum (presumed to be dominated by protons) extends above ~300 keV in energy, then the ions are unlikely to have been accelerated via the Fermi process at the bow shock and are therefore probably of magnetospheric origin [e.g., *Scholer et al*., 1981a; *Sarris et al*., 1987]. In analyzing such high-energy ion events, *Anagnostopoulos et al*. [1986, 1987] had estimated that the He contribution to a spectrum of index $\gamma$ ~5 for a proton-to-alpha ratio of 400 in the 0.05–2 MeV energy range probably does not exceed ~30%; the heavy ion contribution was not considered in this analysis. However, points 5 and 6 above taken together with the proton results discussed in section 6.4, which showed that (1) the spectrum is generally soft with $\gamma$ ~5, and (2) the spectra that did extend above ~0.3 MeV became even softer at higher energies, indicate that the total energy ion spectrum above ~0.3 MeV is essentially dominated by heavy ions during most of the events.

In light of these new results, we suggest that it is necessary to reexamine many of the single parameter ion measurements which showed that the "proton" spectrum in upstream events extended from ~300 keV up to ~2 MeV, and were consequently interpreted as evidence for magnetospheric leakage [e.g., *Anagnostopoulos et al*., 1986, 1987; *Sarris et al*., 1987; *Skoug et al*., 1996]. We note that even though *Skoug et al*. [1996] had recently suggested that the presence of ~2 MeV ions in upstream events was probably due to magnetospheric leakage, they did acknowledge the possibility of an alternative origin if the spectrum at higher energy was dominated by heavier ions. However, we remark that even though our results indicate that the high-energy protons reported in many upstream events were probably heavier ions at lower energy/nucleon, this does not rule out magnetospheric leakage as a plausible mechanism for upstream events (see below).

Furthermore, it is also necessary to reevaluate measurements that showed higher-energy protons (290–550 keV) arriving earlier than those at lower energy and were consequently assumed to exhibit normal velocity dispersion [e.g., *Anagnostoupulos et al*., 1995, 1999]. Since the Fermi model predicts inverse velocity dispersion [e.g., *Scholer*, 1985], such behavior was considered as strong evidence for magnetospheric leakage. However, the respective velocities of a 0.4 MeV proton and a 0.4 MeV CNO ion are ~8800 and ~2200 km s$^{-1}$, while the velocity of a 100 keV proton is ~4400 km s$^{-1}$. Clearly then, total energy ion measurements do not exhibit "normal" velocity dispersion if the lower energy channels measure protons, while the higher-energy channels respond primarily to heavier ions with lower speeds, as evident from the results shown here. On the contrary, it appears that these measurements probably exhibited inverse velocity dispersion. However, we remark that this is also not sufficient to rule out magnetospheric leakage because, depending on the circumstances, the leakage model has often been employed to account for both types of velocity dispersion [*Anagnostopoulos et al*., 1998].

We also note that the time delay between the arrival of the higher and lower energy ions during upstream events that exhibited "normal" velocity dispersion was typically of the order of a few minutes [e.g., *Anagnostoupulos et al*., 1995]. However, a simple scenario in which particles at all energies are released simultaneously into the interplanetary medium followed by propagation out to the location of the spacecraft at ~250 $R_E$ would result in a time delay of <1 min between the arrival of 0.4 and 0.1 MeV protons. To account for the observed normal velocity dispersion, *Anagnostopoulos et al*. [1995] proposed a rigidity-dependent leakage of ions from the magnetosphere, with ions of higher rigidity escaping prior to the lower rigidity ions. The respective rigidities of a 0.4 MeV proton and a 0.4 MeV CNO ion are 27.4 and 18.3 MV, while that of a 100 keV proton is 13.7 MV. Thus, even though the total energy ion measurements were probably misinterpreted as normal velocity dispersion and were consequently elucidated in terms of a rigidity-dependent leakage process, such a mechanism could still, qualitatively, account for the actual inverse velocity dispersion caused by the earlier arrival of 0.4 MeV CNO ions compared with 0.1 MeV protons.

Our results also show that the ion composition in upstream events is similar to typical solar wind values (point 8). To account for the presence of both, the CIR-like heavy ion composition in upstream events and the correlation between the event occurrence rate and the enhancement in both $V_{sw}$ and $K_p$ (see section 7.1 and *Mason et al*. [1996]), *Anagnostopoulos* [1998] has recently proposed that the heavy ions could have been accelerated inside the Earth's magnetosphere and subsequently leaked out into the upstream medium during periods of intense geomagnetic activity. Since high charge state solar wind ions have been observed at spacecraft located inside the Earth's magnetosphere [e.g., *Christon et al*., 1994], and since the onset of geomagnetic activity coincides with the arrival of high-speed solar wind streams [e.g., *Baker et al*., 1994], the above scenario is, at least in a phenomenological sense, consistent with our observations.

However, since the true test of any model is to fit the observations quantitatively, we point out the following challenges (in addition to those discussed in section 7.1) for the leakage model. First, to propose mechanisms responsible for the fractionation and acceleration of the ions observed in the Earth's plasma sheet and the magnetosheath during periods of intense geomagnetic activity (see Table 2) and reproduce the composition and spectra in the upstream events. Second, to reconcile the observation that the event occurrence rate increases almost simultaneously with the appearance of high-speed streams [*Mason et al*., 1996, 1998b] with the corresponding timescales

involved in the acceleration, leakage, and subsequent observation of these ions at Wind.

We have also shown (point 7) that the energy spectra for all species measured during a substantial fraction of the events extended above ~150 and ~230 keV/*e*, which are the upper energy limit of the Fermi acceleration process [e.g., *Lee*, 1982] and the maximum energy observed during a diffuse ion event [*Möbius et al*., 1987], respectively. Ions with energies above ~300 keV/*e* in upstream events were also observed by *Mason et al*. [1996] and *Dwyer et al*. [1997], who surmised that their results were best explained in terms of Fermi acceleration of an already energetic seed population, e.g., from CIRs and SEPs, at the bow shock. Thus it appears that the Fermi mechanism might be able to accelerate ions above ~300 keV/e provided that there exists an energetic seed population available for injection into the process.

To investigate the possible existence of such a seed population in association with the events studied here, we examined the 60 keV/nucleon CNO intensity measured during the preevent time intervals corresponding to all the events. We found that this background intensity exceeded our minimum threshold of 5 particles/(cm$^2$ s sr MeV/nucleon)$^{-1}$ for only ~7% of the events. Thus it appears that the vast majority of the upstream events for which the spectra extended above ~150 keV/*e* could not have been caused by Fermi acceleration of a preexisting energetic (≳40 keV/nucleon) seed population. Although this does not rule out the injection of seed particles with energies ranging from a few keV up to ~40 keV/nucleon, we remark that even if such a superthermal seed population was available, the conditions for Fermi acceleration must remain favorable for a sufficient amount of time (typically well over an hour, see *Ellison et al*. [1990]), to produce the high-energy (≳300 keV/e) events reported here.

Furthermore, we found that the energy spectra for 100–300 keV protons and 30–300 keV/nucleon He, CNO, NeS, and Fe obeyed power laws with $\gamma \sim 3$–5 for ~70% of the events, although the He and CNO spectra for ~30% of the events softened above ~80 keV/nucleon and the proton spectra generally tended to soften above ~300 keV. These results are also at odds with one of the predictions of the Fermi model which states that the energy spectra up to 150 keV/*e* should behave as exponentials because of competition between shock acceleration and putative particle losses. Such losses could occur either due to (1) the finite spatial extent of the bow shock; particles could escape from the shock either via cross-field diffusion [*Lee*, 1982] or acquire high enough energy so that their gyroradii become comparable to the size of the shock [*Eichler*, 1981], and/or (2) particles could propagate beyond a free escape boundary upstream of the shock from where they cannot be convected by the solar wind back into the shock for further acceleration [*Jones and Ellison*, 1991].

Finally, point 3 indicates that 307 events (~25%) were accompanied by 20–48 keV electrons. The presence of ≳30 keV electrons in upstream events is generally considered as evidence for magnetospheric leakage and against Fermi acceleration [e.g., *Scholer et al*., 1981a; *Anagnostopoulos et al*., 1998] because the latter process cannot accelerate electrons owing to their smaller gyroradii and higher speeds. Thus, in addition to the global nature of the source region discussed in section 7.1, any bow shock acceleration model must also account for the power law like behavior of the energy spectra for all species during ~70% of the events. The model must also reconcile the persistent extension of the energy spectra above ~150 keV/e with the time required to accelerate the ions in the absence of an energetic seed population. Finally, the presence of energetic electrons during a substantial fraction of the events must also be explained.

## 8. Summary and Conclusions

We have analyzed the duration times, the electron association, and the energy spectra, anisotropy, and composition of 0.03–2.0 MeV/nucleon ions for 1225 upstream events observed by the EPACT/STEP instrument on board the Wind spacecraft from 1994 day 325 to 1999 day 92. We have also surveyed the temporal and spatial occurrence rates of the events, and the magnetospheric and interplanetary conditions during the events. Our main results are the following:

1. The event occurrence rate showed a clear dependence on the solar cycle.
2. The occurrence rate increased when both $V_{sw}$ and $K_p$ were enhanced.
3. Most events were observed within $\pm 80\ R_E$ in $Y_{GSE}$ and $\sim 100\ R_E$ in $X_{GSE}$, although the events occurred at all locations of the Wind orbit.
4. Approximately 73% of the events were observed when the IMF was radial and in the ecliptic plane and when the spacecraft was most likely magnetically connected to the bow shock.
5. The events typically lasted between 10 min to 3 hours and exhibited strong sunward field-aligned flow.
6. At least 25% of the events were accompanied by 20–48 keV electrons (as measured by the 3DP instrument).
7. The energy spectra of 100–300 keV protons and 30–300 keV/nucleon He-Fe during ~70% of the events obeyed power laws with $\gamma$ between 3 and 5, while the energy spectra of He and CNO for ~30% of the events softened above ~80 keV/nucleon.
8. The total energy ion spectrum above ~0.5 MeV was dominated by heavier ions during the events.
9. A substantial fraction of the spectra (≳75% for protons, He, and CNO and ≳40% for NeS and Fe) extended above ~150 keV/e.
10. The ion composition during the events was similar to typical solar wind values.

We suggest that the temporal changes in the occurrence rate of upstream events and its correlation with $V_{sw}$ and $K_p$ are probably related to changes in the solar cycle. The solar-wind-like ion composition, the heavy ion dominance of the total energy ion spectrum above ~0.5 MeV, the lack of a significant time delay between the arrival of high-speed streams at ~1 AU and the increase in the event occurrence rate, and the fact that the majority of the events were observed in the dawn-noon sector appear to pose severe problems for the leakage model. On the other hand, the global nature of the source region, the extension of the energy spectra of all species above ~150 keV/*e* and their power law like behavior between 30–300 keV/nucleon, and the presence of ~35 keV electrons during a substantial fraction of the events appear to pose serious challenges for the Fermi acceleration model.

**Acknowledgments.** We are grateful to the members of the Space Physics Group, Department of Physics at the University of Maryland, and the EPACT instrumentation team at the Goddard Space Flight Center for the construction of the instrumentation. We thank T. R. Sanderson of the European Space Agency for providing the 3DP

electron data. The work at the University of Maryland was supported in part by NASA contract NAS5-30927 and grant NAG 57228.

Janet G. Luhmann thanks Ruth Skoug for her assistance in evaluating this paper.

## References

Anagnostopoulos, G. C., Comment on "Energetic heavy ions observed upstream of the Earth's bow shock by the STEP/EPACT instrument on WIND" by G. M. Mason, J. E. Mazur, and T. T. von Rosenvinge, *Geophys. Res. Lett*., *9*, 1523, 1998.

Anagnostopoulos, G. C., E. T. Sarris, and S. M. Krimigis, Magnetospheric origin of energetic ($E \geq 50$ keV) ions upstream of the bow shock: The October 31, 1977 event, *J. Geophys. Res*., *91*, 3020, 1986.

Anagnostopoulos, G. C., E. T. Sarris, and S. M. Krimigis, Further on the October 31, 1977 upstream event: A response to D. C. Ellison, *J. Geophys. Res*., *92*, 12,461, 1987.

Anagnostopoulos, G. C., E. T. Sarris, and S. M. Krimigis, On the origin of the forward velocity dispersion of ion events observed near the Earth's and Jupiter's bow shock, *Adv. Space. Res*., *16*, 149, 1995.

Anagnostopoulos, G. C., A. G. Rigas, E. T. Sarris, and S. M. Krimigis, Characteristics of upstream energetic ($E \geq 50$ keV) ion events during intense geomagnetic activity, *J. Geophys. Res*., *103*, 9521, 1998.

Anagnostopoulos, G. C., G. Kaliabetsos, G. Argypoulos, and E. T. Sarris, High energy ions and electrons upstream from the Earth's bow shock and their dependence on geomagnetic conditions: Statistical results between years 1982–1988, *Geophys. Res. Lett*., *26*, 2151, 1999.

Arnaud, M., and R. Rothenflug, An updated evaluation of recombination and ionization rates, *Astron. Astrophys. Suppl. Ser*., *60*, 425, 1985.

Asbridge, J. R., S. J. Bame, and I. B. Strong, Outward flow of protons from the Earth's bow shock, *J. Geophys. Res*., *73*, 5777, 1968.

Baker, D. N., J. B. Blake, L. B. Callis, J. R. Cummings, S. Kanekal, B. Klecker, R. A. Mewaldt, and R. D. Zwickl, Relativistic electron acceleration and decay time scales in the inner and outer radiation belts: SAMPEX, *Geophys. Res. Lett*., *21*, 409, 1994.

Christon, S. P., D. C. Hamilton, G. Gloeckler, T. E. Eastman, and F. M. Ipavich, High charge state carbon and oxygen ions in Earth's equatorial quasi-trapping region, *J. Geophys. Res*., *99*, 13,465, 1994.

Christon, S. P., et al., Observation of singly-charged ionospheric oxygen ions at 27 $R_E$ sunward of Earth, *Eos Trans. AGU*, *80*(17), 297, 1999.

Dwyer, J. R., G. M. Mason, J. E. Mazur, and T. T. von Rosenvinge, Acceleration of solar flare $^3$He at the Earth's bow shock, *Geophys. Res. Lett*., *24*, 61, 1997.

Dwyer, J. R., G. M. Mason, M. I. Desai, J. E. Mazur, and T. T. von Rosenvinge, The spatial structure of ion events measured upstream of the Earth's bow shock by ACE/ULEIS and WIND/STEP, *Geophys. Res. Lett*., in press, 1999.

Eichler, D., Energetic particle spectra in finite shocks: The Earth's bow shock, *Astrophys. J*., *244*, 711, 1981.

Ellison, D. C., E. Möbius, and G. Paschmann, Particle injection and acceleration at Earth's bow shock: Comparison of upstream and downstream events, *Astrophys. J*., *352*, 376, 1990.

Gloeckler, G., and D. C. Hamilton, AMPTE ion composition results, *Phys. Scr*., *T18*, 73, 1987.

Gosling, J. T., J. R. Asbridge, S. J. Bame, G. Paschmann, and N. Sckopke, Observations of two distinct populations of bow shock ions in the upstream solar wind, *Geophys. Res. Lett*., *5*, 957, 1978.

Haggerty, D. K., et al., Simultaneous observations of energetic (~150 keV) protons upstream of the Earth's bow shock at ACE and WIND, *Geophys. Res. Lett*., *26*, 169, 1999.

Ipavich, F. M., The Compton-Getting effect for low energy particles, *Geophys. Res. Lett*., *1*, 149, 1974.

Ipavich, F. M., A. B. Galvin, G. Gloeckler, M. Scholer, and D. Hovestadt, A statistical survey of ions observed upstream of the Earth's bow shock: Energy spectra, composition, and spatial variation, *J. Geophys. Res*., *86*, 4337, 1981a.

Ipavich, F. M., M. Scholer, and G. Gloeckler, Temporal development of composition, spectra, and anisotropies during upstream particle events, *J. Geophys. Res*., *86*, 11,153, 1981b.

Jones, F. C., and D. C. Ellison, The plasma physics of shock acceleration, *Space Sci. Rev*., *58*, 259, 1991.

Krimigis, S. M., D. Venkatesan, J. C. Barichello, and E. T. Sarris, Simultaneous measurements of energetic protons and electrons in the distant magnetosheath, magnetotail, and upstream in the solar wind, *Geophys. Res. Lett*., *5*, 961, 1978.

Lee, M. A., Coupled hydromagnetic wave excitation and ion acceleration upstream of the Earth's bow shock, *J. Geophys. Res*., *87*, 5063, 1982.

Lepping, R. P., et al., The WIND magnetic field investigation, *Space Sci. Rev*., *71*, 207, 1995.

Lin, R. P., C. I. Meng, and K. A. Anderson, 30- to 100 keV protons upstream from the Earth's bow shock, *J. Geophys. Res*., *79*, 489, 1974.

Lin, R. P., et al., A three-dimensional plasma and energetic particle investigation for the WIND spacecraft, *Space Sci. Rev*., *71*, 125, 1995.

Mason, G. M., J. E. Mazur, and T. T. von Rosenvinge, Energetic heavy ions observed upstream of the Earth's bow shock by the STEP/EPACT instrument on WIND, *Geophys. Res. Lett*., *23*, 1231, 1996.

Mason, G. M., J. E. Mazur, J. R. Dwyer, D. V. Reames, and T. T. von Rosenvinge, New spectral and abundance features of interplanetary heavy ions in corotating interaction regions, *Astrophys. J*., *486*, L149, 1997.

Mason, G. M., et al., The ultra-low-energy isotope spectrometer (ULEIS) for the ACE spacecraft, *Space Sci. Rev*., *86*, 409, 1998a.

Mason, G. M., J. E. Mazur, and T. T. von Rosenvinge, Reply to comment by G. C. Anagnostopoulos on "Energetic heavy ions observed upstream of the Earth's bow shock by the STEP/EPACT instrument on WIND" by G. M. Mason, J. E. Mazur, and T. T. von Rosenvinge, *Geophys. Res. Lett*., *9*, 1527, 1998b.

Mitchell, D. G., and E. C. Roelof, Dependence of 50-keV upstream ion events at IMP 7 & 8 upon magnetic field bow shock geometry, *J. Geophys. Res*., *88*, 5623, 1983.

Mitchell, D. G., E. C. Roelof, T. R. Sanderson, R. Reinhard, and K.-P. Wenzel, ISEE/IMP observations of simultaneous upstream ion events, *J. Geophys. Res*., *88*, 5635, 1983.

Möbius, E., D. Hovestadt, B. Klecker, M. Scholer, F. M. Ipavich, C. W. Carlson, and R. P. Lin, A burst of energetic $O^+$ ions during an upstream particle event, *Geophys. Res. Lett*., *13*, 1372, 1986.

Möbius, E., M. Scholer, N. Sckopke, H. Lühr, G. Paschmann, and D. Hovestadt, The distribution function of diffuse ions and the magnetic field power spectrum upstream of the Earth's bow shock, *Geophys. Res. Lett*., *14*, 681, 1987.

Ogilvie, K. W., et al., SWE, A comprehensive plasma instrument for the WIND spacecraft, *Space Sci. Rev*., *71*, 55, 1995.

Reames, D. V., Particle acceleration at the Sun and in the heliosphere, *Space Sci. Rev*., in press, 1999.

Sanderson, T. R., R. Reinhard, and K.-P. Wenzel, The propagation of upstream protons between the Earth's bow shock and ISEE 3, *J. Geophys. Res*., *86*, 4425, 1981.

Sanderson, T. R., et al., WIND observations of energetic ions far upstream of the Earth's bow shock, *Geophys. Res. Lett*., *23*, 1215, 1996.

Sanderson, T. R., et al., WIND observations of the influence of the Sun's magnetic field on the interplanetary medium at 1 AU, *J. Geophys. Res*., *103*, 17,235, 1998.

Sarris, E. T., S. M. Krimigis, and T. P. Armstrong, Observations of magnetospheric bursts of high energy protons and electrons at 35 $R_E$ with IMP 7, *J. Geophys. Res*., *81*, 2341, 1976.

Sarris, E. T., S. M. Krimigis, C. O. Bostrom, and T. P. Armstrong, Simultaneous multispacecraft observations of energetic proton bursts inside and outside the magnetosphere, *J. Geophys. Res*., *83*, 4289, 1978.

Sarris, E. T., G. C. Anagnostopoulos, and S. M. Krimigis, Simultaneous measurements of energetic ion (≥50 keV) and electron (≥220 keV) activity upstream of Earth's bow shock and inside the plasma sheet: Magnetospheric source for the November 3 and December 3, 1977 upstream events, *J. Geophys. Res*., *92*, 12,083, 1987.

Scholer, M., Diffusive acceleration, in *Collisonless Shocks in the Heliosphere*, *Geophys. Monogr. Ser*., vol. 35, edited by B. T. Tsurutani and R. G. Stone, p. 287, AGU, Washington, D.C., 1985.

Scholer, M., G. Gloeckler, F. M. Ipavich, D. Hovestadt, and B. Klecker, Pitch angle distributions of energtic protons near the Earth's bow shock, *Geophys. Res. Lett*., *6*, 707, 1979.

Scholer, M., F. M. Ipavich, G. Gloeckler, D. Hovestadt, Conditions for acceleration of energetic ions ≳30 keV associated with the Earth's bow shock, *J. Geophys. Res*., *85*, 4602, 1980.

Scholer, M., D. Hovestadt, F. M. Ipavich, and G. Gloeckler, Upstream

energetic ions and electrons: Bow shock-associated or magnetospheric origin, *J. Geophys. Res*., *86*, 9040, 1981a.

Scholer, M., F. M. Ipavich, G. Gloeckler, and D. Hovestadt, Simultaneous observations of energetic protons close to the bow shock and far upstream, *J. Geophys. Res*., *49*, 186, 1981b.

Scholer, M., E. Möbius, L. M. Kistler, and F. M. Ipavich, Correlated observations of energetic particles upstream of the bow shock, in the magnetosheath, and in the magnetosphere, *J. Geophys. Res*., *95*, 21,297, 1990.

Sibeck, D., and R. W. McEntire, Multiple satellite observations of leakage of particles from the magnetosphere, *Adv. Space. Res*., *8*(9), 210, 1988.

Skoug, R. M., et al., Upstream and magnetosheath energetic ions with energies to ≈2 MeV, *Geophys. Res. Lett*., *23*, 1223, 1996.

Sonnerup, B. U. Ö., Acceleration of particles reflected at a shock front, *J. Geophys. Res*., *74*, 1301, 1969.

Stansberry, J. A., J. T. Gosling, M. F. Thompsen, S. J. Bame, and E. J. Smith, Interplanetary magnetic field orientations associated with bidirectional electron heat fluxes detected at ISEE-3, *J. Geophys. Res*., *93*, 1975, 1988.

von Rosenvinge, T. T., L. M. Barbier, J. Karsch, R. Liberman, M. P. Ladden, et al., The energetic particle: Acceleration, composition, and transport (EPACT) investigation on the WIND spacecraft, *Space Sci. Rev*., *71*, 155, 1995.

von Steiger, R., J. Geiss and G. Gloeckler, Composition of the solar wind, in *Cosmic Winds and the Heliosphere*, edited by J. R. Jokipii, C. P. Sonnet, and M. S. Giampapa, Arizona Press, Tucson, 1997.

---

M. I. Desai, J. R. Dwyer, and G. M. Mason, Department of Physics, University of Maryland, College Park, MD 20742. (desai@uleis.umd.edu)

R. P. Lepping and T. T. von Rosenvinge, NASA Goddard Space Flight Center, Greenbelt, MD 20771.

J. E. Mazur, Aerospace Corporation, Los Angeles, CA 90009.

(Received June 18, 1999; revised August 31, 1999;
accepted August 31, 1999.)